Available online at www.sciencedirect.com
SCIENCE DIRECT®
Control Engineering Practice 13 (2005) 383–398
CONTROL ENGINEERING PRACTICE
www.elsevier.com/locate/conengprac

Design and flight testing of various $\mathscr{H}^\infty$ controllers for the Bell 205 helicopter

Ian Postlethwaite[a,1], Emmanuel Prempain[a,1,2], Ercument Turkoglu[a,1], Matthew C. Turner[a,*,1], Kris Ellis[b], A.W. Gubbels[b]

[a] *Control and Instrumentation Group, Department of Engineering, University of Leicester, Leicester, UK*
[b] *Flight Research Laboratory, Institute of Aerospace Research, National Research Council of Canada, Ottawa, Ont., Canada K1A 0R6*

Received 4 February 2003; accepted 8 December 2003

Abstract

This paper describes the flight testing of a suite of $\mathscr{H}^\infty$ controllers designed using linearisations extracted from a *new* nonlinear model of the Bell 205 helicopter. Details of the controller designs are presented, together with a comprehensive analysis of simulation and flight-test results. These are complemented by an evaluation of qualitative and quantitative handling qualities information against the design standard ADS-33. The most notable achievements of the work were: (1) stability was achieved for all controllers tested and, moreover, some of them yielded desirable handling qualities from the first test onwards, and (2) a high degree of consistency between desk-top simulation and flight-test results was observed. Achieved performance was generally satisfactory and future planned flight tests will build on these results with the aim to increase performance further. The paper discusses various aspects of controller design and presents an analysis of the results obtained. The likely direction of further work is also discussed.

Keywords: Flight control; H-infinity control; Helicopter control; Robust control

1. Introduction

Helicopters are a difficult type of aircraft to control: generically they exhibit a complex, nonlinear dynamic behaviour and are subject to a high degree of inter-axis coupling. In addition, helicopters are open-loop unstable and most mathematical models contain a moderate-high degree of uncertainty associated with neglected dynamics and poorly understood aero-mechanical couplings. It is also important to mention that the Bell 205 aircraft studied here has teetering rotor dynamics, tight actuator rate-limits, and computational delays which combine to form something akin to a large time delay in all channels at the plant input. These delays, along with right-half-plane poles and right-half-plane zeros set stringent bounds on the achievable sensitivity and co-sensitivity functions, placing an upper bound on the achievable bandwidth. Ultimately this limits the performance which can be extracted from the aircraft, irrespective of the controller design method.

During the execution of certain manoeuvres and in the presence of degraded visual or operational conditions (such as fog or high winds, for example), the pilot often has to concentrate intensely to obtain even satisfactory task performance. This is due to the aforementioned complex behaviour of the helicopter and, particularly, its multi-axis nature. To relieve the pilot of some of this workload, and to increase the level of task performance, some sort of automatic control augmentation is needed. Stringent requirements for military rotorcraft have been documented in Anonymous (2000), which sets out requirements of control systems in order to achieve adequate de-coupling, stability and manoeuvrability.

A design procedure well suited to the control of helicopters is the technique of $\mathscr{H}^\infty$ control. Being an inherently multivariable technique and also being able to provide robust stability for systems subject to uncertainty make it an ideal candidate. In fact the application of $\mathscr{H}^\infty$ techniques to helicopters has reached a fairly mature stage, progressing over the past

*Corresponding author. Tel.: +44-116-252-2548; fax: +44-116-252-2619.
E-mail address: mct6@sun.engg.le.ac.uk (M.C. Turner).
[1] Research supported by the UK Engineering and Physical Sciences Research Council.
[2] Now with the Department of Electrical Engineering and Electronics, University of Liverpool, Liverpool, UK.

0967-0661/$ - see front matter © 2004 Elsevier Ltd. All rights reserved.
doi:10.1016/j.conengprac.2003.12.008

Nomenclature

$\psi_{heading}$	heading angle (yaw attitude)
θ, ϕ	pitch and roll attitudes
p, q, r	angular velocity components about X, Y and Z axes
u, v, w	translational velocity components along X, Y and Z axes
ψ	rotor blade azimuth angle
Ω	main rotor rotational speed
$\lambda_0, \lambda_{1c}, \lambda_{1s}$	rotor uniform and first harmonic inflow velocities
$\beta_0, \beta_{1c}, \beta_{1s}$	rotor blade coning, longitudinal and lateral flapping angles
$\dot{\beta}_0, \dot{\beta}_{1c}, \dot{\beta}_{1s}$	rotor blade coning, longitudinal and lateral flapping rates
$\theta_0, \theta_{1c}, \theta_{1s}$	main rotor collective, longitudinal and lateral cyclic pitch angles
$\dot{\theta}_0, \dot{\theta}_{1c}, \dot{\theta}_{1s}$	main rotor collective, longitudinal and lateral cyclic pitch rates
Q_e, $\dot{Q}_e$	engine torque and engine torque rate
β_d, $\dot{\beta}_d$	differential coning flap coordinate and rate
δ_{tr}, $\dot{\delta}_{tr}$	tail rotor collective pitch angle and rate
$\gamma > 0$	achievable bound on the $\mathscr{H}^\infty$ norm of generalised plant

decade from simulation to flight test. The work began with Tombs (1987) (see also Yue & Postlethwaite, 1990) where the S/KS $\mathscr{H}^\infty$ mixed-sensitivity technique was applied to the Westland Lynx helicopter; this line of research was continued in Walker and Postlethwaite (1996) where $\mathscr{H}^\infty$ loop-shaping techniques were used, also on the Lynx aircraft. In 1996, the University of Leicester and the National Research Council of Canada's (NRC) Flight Research Laboratory began collaborating on the advanced control of the NRC's Bell 205 helicopter: and in 1997 (see Postlethwaite et al. (1999)), the first $\mathscr{H}^\infty$ controller was tested successfully in-flight, leading to several further successful flight tests. The work of Postlethwaite et al. (1999) again used the $\mathscr{H}^\infty$ loop-shaping technique and provided upper *Level* 2 handling qualities. An alternative mixed-sensitivity S/KS series of controllers was reported in Walker, Turner, Smerlas, Gubbels, and Strange (1999).

This paper builds on the foregoing work in several ways. Firstly, it uses an improved nonlinear flight mechanic model for the basis of design and simulation. Secondly, for the purposes of simulation and analysis, this model is augmented with several extra elements such as time delays, anti-aliasing filters, rate-limits, discretisation and, to reflect the finite precision implementation, the controller realisations are truncated to between six and eight decimal places. Also, extra care was taken to ensure that robustness was achieved for uncertainties greater than expected; for example controllers were routinely checked for robustness of up to 0.08 s in computational delay, when the expected delay was roughly half that. The aim behind these improved simulation techniques was to provide extra closed-loop robustness and to ensure that simulation and flight test were as close as possible to each other.

The paper is organised as follows. Section 2 discusses, briefly, the physical helicopter, while Section 3 describes the design methods used for controller synthesis. Section 4 presents results from simulation and flight-tests and also gives a short ADS-33 evaluation. Some concluding remarks are given in Section 5.

2. Physical helicopter

For control purposes, the helicopter can be thought of, roughly, as a four axis vehicle, the axes to be controlled being vertical, longitudinal, lateral and directional. The helicopter exhibits an approximate *diagonally dominant* structure meaning that each axis is primarily influenced by a certain control effector, although significant cross-coupling exists between all axes. This relationship is summarised in Table 1. Note that without some appropriate decoupling (be this static, dynamic or a mixture of the two) the resulting behaviour of the helicopter can be poor and the pilot workload high.

This study is focused on the Bell 205 helicopter operated by the National Research Council of Canada's (NRC) Flight Research Laboratory in Ottawa. This helicopter exhibits the standard multi-axis behaviour common to most helicopters, but also has the drawback of possessing a teetering rotor, which does not allow as much control power to be generated compared, for example, to a semi-rigid rotor system. In addition the dynamics of such a rotor place a phenomenon in the forward path of the open-loop system, which, in control terms, can be thought of as a pure time delay; this limits the bandwidth achievable in the system.

Table 1
Control effectors

Effector	Axis primarily influenced	Controlled variable
Main rotor collective (θ_0)	Height	N/A
Longitudinal cyclic (θ_{1s})	Longitudinal	Pitch attitude (θ)
Lateral cyclic (θ_{1c})	Lateral	Roll attitude (ϕ)
Tail rotor collective (δ_{tr})	Directional	Yaw rate (r)

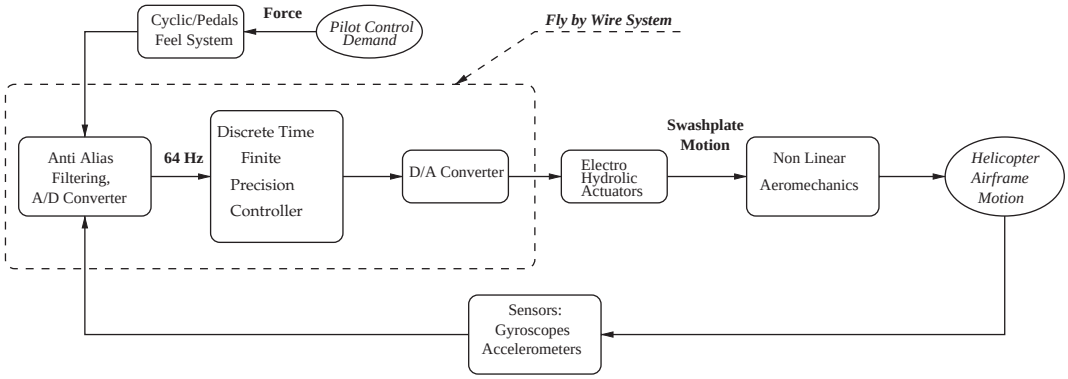

Fig. 1. Schematic helicopter representation.

Fig. 1 shows a schematic of the operation of the helicopter, with the following key components:

- *Nonlinear aeromechanics*: The nonlinear dynamics of the Bell 205 are represented mathematically by a 12 degree-of-freedom (DoF) model, originating from the generic helicopter model, HELISIM Padfield (1981), developed at QinetiQ (formerly DERA). In recent years, to capture suitably the behaviour of the Bell 205 aircraft and to accommodate recent improvements and lessons learned in various flight tests, this model has been modified by Strange and Howitt (1998) and Howell and McCallum (2001).

  The dynamic model in use approximates the fuselage as a rigid body possessing 6 DoF: three translational and three rotational. The main rotor and the tail rotor components are both of teetering type, each configured with rigid and constant-in-length two chord blades attached to the rotating axis. The structure of the rotor allows no transfer of moments to the hub, and all structural moments remain internal. The main rotor is treated as of blade element type. However, the anti-torque tail rotor, operating in quasi-steady form, is represented using a rotor disk model. The fuselage aerodynamic data within DERA Helisim is described by a combination of polynomial functions and one-dimensional look-up tables to give aerodynamic loads *D*rag and *L*ift as a function of local incidence α_i and side slip β. The same method has been adopted for the fin and tail plane, where tail–fin blockage and tail–rotor root cut-out scale factors Prouty (1995) have also been included. The mathematical model of the helicopter also accommodates advancing and regressing flap and conning degrees of freedom. The wake created by the main rotor, called dynamic inflow, is a representation of the flow at the rotor disk in terms of a finite number of inflow states. A dynamic inflow mathematical model Peters and HaQuang (1988) of 3 DoF is included to represent the inflow at any point on the rotor disk as a combination of uniform and first harmonic components, that yield the time-varying induced flow parallel to the rotor shaft.
- *Sensors and A/D converters*: The measurements used for the controller designs described here were recorded using mechanical gyroscopes which were then anti-alias filtered by second-order butterworth filters with 10 Hz cut-off, prior to being sampled at 64 Hz.
- *Controller*: For implementation, the control laws were discretised using Tustin's algorithm and their state–space realisations truncated to between five and eight decimal places. Due to limitations of the on-board computer which ran the control algorithms there was an upper bound on the number of states which the controllers could contain. We found that a 30-state controller could be accommodated satisfactorily. The on-board C-compiler also limited the size of the truncated measurements to about eight decimal places. Truncations of less than five decimal places led to deteriorated response types, but five or greater decimal place truncations seemed adequate for our controllers. The flight control computer was able to operate using floating-point arithmetic.
- *D/A conversion*: The control signal was converted to an analogue signal to drive the actuators using a zero-order hold.
- *Actuators*: The actuators were modelled as second-order transfer functions with saturations in both magnitude and rate. The rate saturation, in degrees/s was highly uncertain but thought to be approximately 1.5 times the magnitude limit of the actuator in degrees, the magnitude limits ranging from 7.5° to 20.5° full scale deflection.
- *Stick and feel system*: The NRC Bell 205 Airborne Simulator employs an artificial force feel system to restore inceptor force and position cues to the pilot. This system includes a hydraulically driven cyclic centre stick and pedals with integrated strain gauge bridges to sense pilot applied forces. The measured forces are converted to digital at 600 Hz and processed by a VME computer employing a model

following technique to perform control loop closure on the hydraulic servo actuators. This arrangement allows the user to select the desired feel system properties including linear characteristics such as inertia, spring gradient, and damping, as well as nonlinear elements such as friction (dynamic and static), breakouts, and notches. The system is further described by Gubbels and Goheen (1997).

All $\mathscr{H}^\infty$ controller testing described in this paper was performed with a moderate spring gradient feel system with good cyclic centreing characteristics. Inertia, spring gradient, and damping were subjectively tuned to resemble the control feel of a Westland Lynx. Measured control force was only employed as an input to the artificial feel system, whereas the $\mathscr{H}^\infty$ controller used control displacement as its input.

The role of the feel system in the calculation of bandwidth and phase delay is not currently well understood, Hoh, Nitchell and Aponso (1989). There is debate over whether the feel system dynamics of a position sensing flight control system should be included in the calculation of aircraft response bandwidth and phase delay, or treated separately. Nevertheless, the influence of the feel system dynamics can be significant; for example, an overdamped and high inertia feel system married to an otherwise high bandwidth flight controller will result in poor handling qualities with pilot complaints similar to those of a low bandwidth flight control system.

3. Controller design strategies

3.1. $\mathscr{H}^\infty$ control

All the controllers described in this paper were designed using $\mathscr{H}^\infty$ frequency domain-based optimisation techniques, which are deemed useful in the context of helicopter flight control due to their ability to cope with uncertainties and their inherently multivariable nature. The goal of $\mathscr{H}^\infty$ control theory is to minimise the $\mathscr{H}^\infty$ norm of a certain closed-loop transfer function matrix which is chosen to enforce various desirable closed-loop attributes. Roughly speaking making the $\mathscr{H}^\infty$ norm of transfer functions small, corresponds to making the energy gain, or equivalently, the maximum gain across all frequency, small. Uncertainties are handled by making the $\mathscr{H}^\infty$ norm of certain transfer functions small for certain frequency ranges; performance can be accommodated by making the $\mathscr{H}^\infty$ norm of other transfer functions small during other frequency ranges. This results in a design goal of finding a controller $K(s)$ such that the $\mathscr{H}^\infty$ norm of a certain closed-loop transfer function $T_{zw}(K, G)$ is minimised, or at least lower than a certain bound. Embedded within the transfer function matrix T_{zw} are the individual transfer functions which we would like to minimise for robustness/performance purposes (e.g. sensitivity, co-sensitivity). A full description of $\mathscr{H}^\infty$ control is beyond the scope of this paper and the interested reader is referred to Skogestad and Postlethwaite (1996) for a more thorough treatment of this topic.

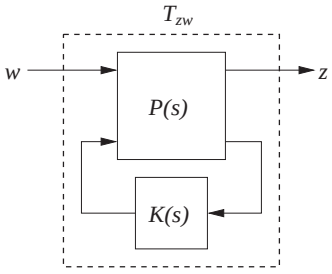

Fig. 2. $\mathscr{H}^\infty$ control problem.

A pictorial representation of the general $\mathscr{H}^\infty$ problem is shown in Fig. 2. Here the matrix $P(s)$ represents the interconnection structure between, the actual plant $G(s)$, any designed specified weights, $W_i(s)$, $i = \{1, 2, \ldots\}$ and the inputs and outputs. The vector w contains all exogenous inputs which represent disturbances, uncertainties, etc., some of which may be fictitious but useful for design. The vector z contains all signals which we require to be minimised. Standard software, such as the Matlab μ Analysis and Synthesis Toolbox, can be used to solve this problem sub-optimally i.e. find a controller $K(s)$ which ensures $\|T_{zw}\|_\infty < \gamma$ for some sufficiently small γ.

3.2. Design model

The basis for controller design was a 32-state nonlinear flight mechanic model of the Bell 205, provided by QinetiQ (formerly DERA) Bedford. The model integrates 9-states describing the rigid-body dynamics of the helicopter fuselage, 3-states representing the dynamic inflow on the main rotor, 8-states governing the rotor flapping motions of the non-rotating frame, 8-states describing engine and main rotor actuator dynamics, 2-states representing rotor position and angular velocity (ψ, Ω), and 2-states mapping the dynamics of the tail rotor servo.

The periodic nature of the equations of motion of the system required it to be trimmed using the McVicar and Bradley (1997) trimming algorithm, which was followed by linearisation at 30 ft/s forward airspeed, level flight. To prevent high-order controllers and to ease the process of synthesis and implementing of the resulting controllers, this model was first truncated, by inspection, to 29 states. The states removed by truncation were uniform inflow (λ_0), rotor azimuth (ψ) and heading ($\psi_{heading}$), respectively. Heading ($\psi_{heading}$), an independent mode

from the short period stabilization problem was removed, partly because it is discontinuous at modulo 2π radians, and partly as it can be expressed in terms of the rigid body states and θ and ϕ. The 29-state model was then residualised to 13 states retaining the dominant rigid-body dynamics (i.e. the states θ, ϕ, u, v, w, p, q, r) and retaining the salient main and tail rotor actuator dynamics (i.e. the states θ_{1c}, θ_{1s}, $\dot{\theta}_{1c}$, $\dot{\theta}_{1s}$, δ_{tr}). The residualized states were mainly those associated with the rotors, which could be replaced with their steady-state values. Fig. 3 depicts the original (nominal) plant and the truncated-residualised model plant singular values.

The choice of the model reduction methods and the selection of appropriate modes in the model reductions are beyond the frame of the paper. For more details the reader is referred to Skogestad and Postlethwaite (1996) and Padfield (2000), respectively, as well as the references therein.

Inspecting the singular values in Fig. 3 clearly reveals that the plant has a high condition number at some frequencies, reflecting on its sensitivity to a relative change (or error) in itself. Examination of Tables 2 and 3 discloses some other undesirable characteristics of the open-loop model, namely, the presence of unstable (right-half-plane) poles and zeros. Their natural frequencies place lower and upper bounds on the closed-loop bandwidth of each channel. It was observed that the first right-half-plane zero, being almost at the origin, prevented effective integral action in the yaw channel.

Several types of controller were designed for the Bell 205. It must be noted that, for their synthesis, the controllers presented herein used the same reduced (truncated-residualized) linear-time-invariant-finite-dimensional model of the rotary-wing aircraft and were designed principally around a body axis referenced low forward speed of 30 feet/s linearisation. All were three

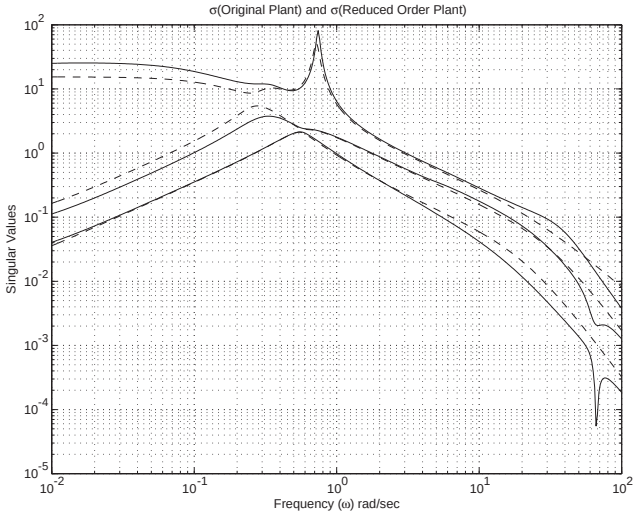

Fig. 3. Singular values of original (solid) and reduced (dashed) plant.

Table 2
Open-loop unstable poles

Poles		Undamped natural frequency	Damping ration
Real	Imaginary		
1.0906e − 001	−3.25e − 001	3.4282e − 001	−3.1814e − 001
1.0906e − 001	3.25e − 001	3.4282e − 001	−3.1814e − 001

Table 3
Open-Loop unstable zeros

Zeros		Undamped natural frequency	Damping ratio
Real	Imaginary		
7.3088e − 003	0.0000e + 000	7.3088e − 003	−1.0000e + 000
3.9062e − 002	−6.6630e + 001	6.6630e + 001	−5.8625e − 004
3.9062e − 002	6.6630e + 001	6.6630e + 001	−5.8625e − 004

axis control laws: the pitch, roll and yaw axes were controlled with the collective channel left open-loop (this was partly due to safety reasons and partly due to pilot preference as this channel is stable). All controllers had three control channels: the longitudinal and lateral cyclic to control pitch and roll manoeuvres, respectively, and tail rotor collective to control yaw. The controlled outputs were θ, ϕ, r, and the measured outputs were θ, ϕ, r, p, q.

3.3. Two degree of freedom full information controllers

The 2 DOF controller is made of two elements which can be designed separately. Fig. 4 shows the structure considered. The signals $u \in R^{n_u}$ and $y \in R^{n_y}$ denote the control input vector and the measured output vector, respectively, while $r \in R^{n_r}$ denotes the reference command. K_2 is the feedback regulator which is used to stabilise and to ensure a certain level of decoupling. T_F is the feedforward filter. T_F is designed from the state space linearised model of the helicopter. The role of T_F is to improve tracking by generating the desired (ideal) output (y_m) and control input (u_m) signals which must be tracked by the feedback part. Feedforward and feedback parts are interconnected through

$$J := \left[\begin{array}{ccc|c} 0 & I_{n_u} & 0 & -I_{n_u} \\ \hline -I_{n_y} & 0 & I_{n_y} & 0 \end{array}\right]$$

to form a 2 DOF controller. The feedforward filter T_F is usually designed via a state-feedback or a full information synthesis. For more details about this control structure the reader is referred to Prempain and Postlethwaite (2001). A major advantage of this control structure is that one can make use of an existing

feedback regulator (already flight tested) with a T_F to improve tracking. This is a good way to test a new controller with the insurance of acceptable (e.g. at least stable) responses, obtained from the first flight test. Then, when a good T_F is designed, a new feedback regulator K_2 can be designed to improve performance robustness.

3.3.1. The existing PI feedback regulator

The actual Bell 205 is fitted with a simple PI regulator (K_2 in Fig. 4) which results from several ad hoc in-flight tunings. K_2 does not use the direct measurement of the rate signals (p, q, r). Indeed K_2 is driven with mixed rate signals which are composite signals consisting of low-frequency components from the measured rates, together with high-frequency components generated from a linear model of the helicopter.

Mixed rate feedback can be considered as an ad hoc technique used to reduce the bandwidth of the closed loop by adding extra lag at high frequencies (Baillie, Morgan, & Goheen, 1995).

The output-sensitivity for the longitudinal and lateral axes is shown in Fig. 5. This plot is quite different from what one may expect from an academic point of view. Disturbance rejection is very poor at low frequencies. Thus, the co-sensitivity function $T_i = K_2G(I - K_2G)^{-1}$ does not tend to identity at DC and therefore it is difficult to predict any good decoupling or tracking properties from this plot. The corresponding linear time responses for unit step demands in each axis are given in Fig. 6.

Clearly, the decoupling is poor and the tracking is sluggish. The main merit of the PI regulator is to stabilise the plant across the entire flight envelope with extremely gentle control signals (low bandwidth control).

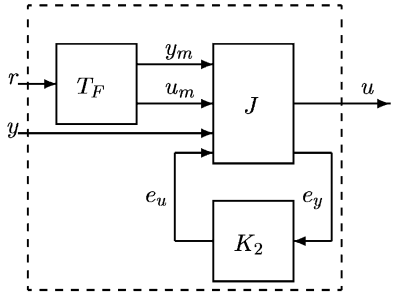

Fig. 4. Two DOF controller structure.

3.3.2. Feedforward synthesis

The feedforward filter is based on a full-information $\mathscr{H}^\infty$ synthesis based on the interconnection given in Fig. 7. For simplicity, in this application, the reference model T_M has been selected as the identity matrix and the selector matrix as $E = [I_3\ 0_{3\times 2}]$. W_1 is used for tracking accuracy and is chosen as a high-gain low-pass filter. It ensures a tracking error less than $\frac{1}{20}$ at DC. The bandwidth is limited by the weighting function W_2, which is chosen as a high pass filter.

3.4. De-coupled controllers

One of the conclusions of Walker et al. (1999) was that, due to possibly poor modelling of the longitudinal–lateral channel interactions, a longitudinal–lateral decoupled control scheme could perform well. Indeed, the results of Walker et al. (1999) showed the pilot detected little or no coupling during flight tests, and the results obtained in this manner were some of the most promising $\mathscr{H}^\infty$ results obtained on the Bell 205. One of the main drawbacks of the controllers designed in Walker et al. (1999) was that in order for them to

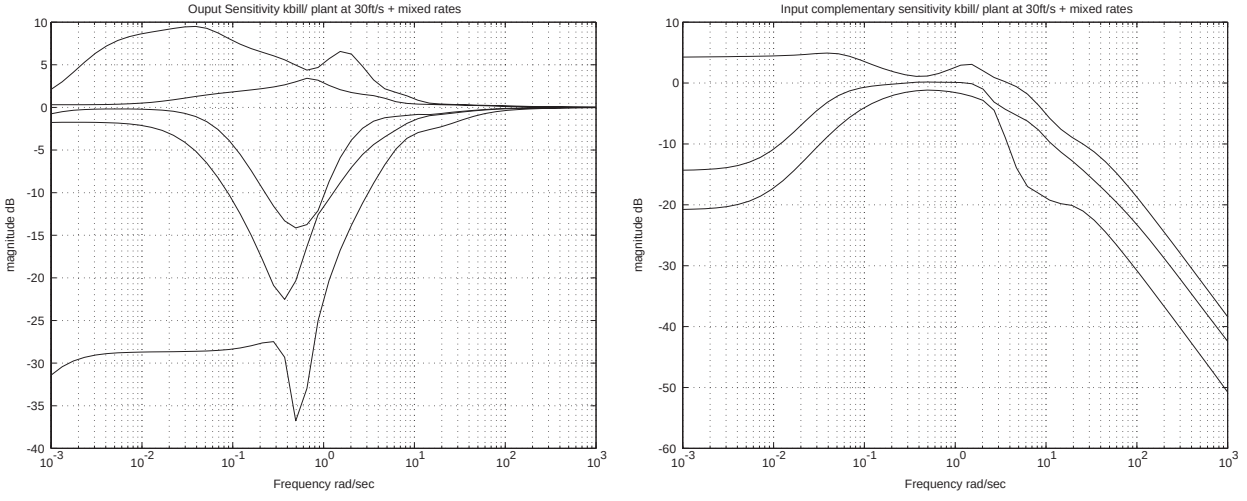

Fig. 5. PI regulator with mixed rate feedback: S_o and T_i.

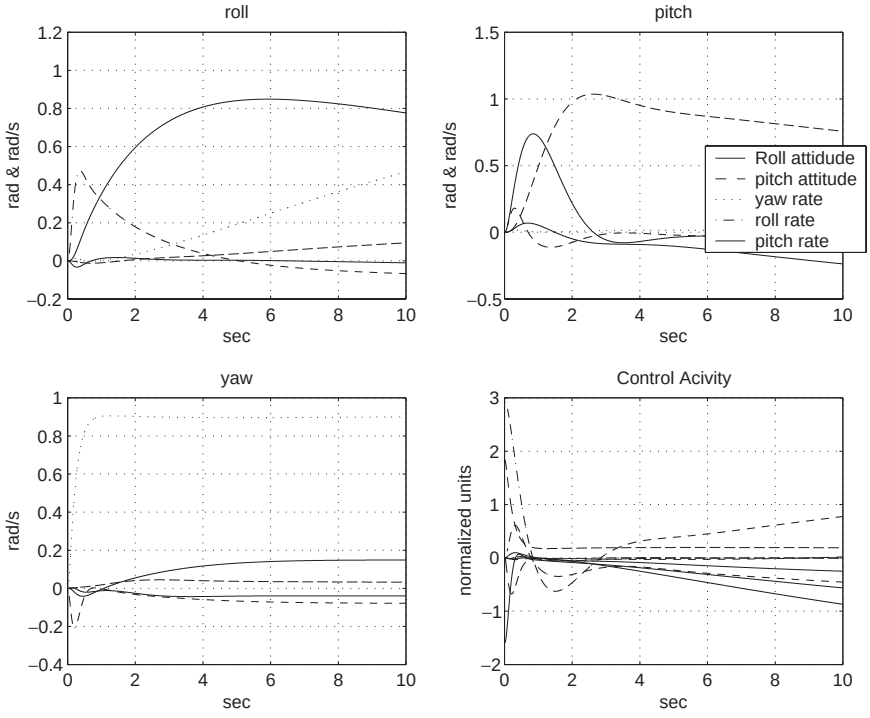

Fig. 6. Nominal unit step responses.

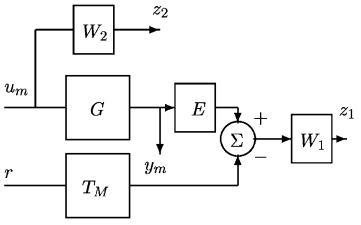

Fig. 7. Open-loop interconnection structure for the feedforward filter design.

function correctly (i.e. to ensure closed-loop stability) they used the *mixed-rate* feedback described earlier. Although this was necessary in the 2 DOF controllers described earlier, due to their reliance on the pre-synthesised feedback part, in principle mixed rates should not be required by $\mathscr{H}^\infty$ controllers.

For this set of flight tests the same idea as Walker et al. (1999) was used for controller design: decoupled designs would be performed with one controller designed purely for pitch control (longitudinal cyclic to θ, q) and one controller designed for lateral control (lateral cyclic and tail rotor collective to ϕ, r, p). However, as one of the principal goals of mixed rate feedback is to increase tolerance to time delays by lowering the frequency at which the gain begins to roll-off, it was decided not to use mixed rate-feedback but to use the $\mathscr{H}^\infty$ weighting functions to carefully shape the frequency response of the system to guard against time delays.

Several different designs were implemented on the aircraft; the one described here is one of the more successful–essentially an $\mathscr{H}^\infty$ 2 DOF loop shaping (Limebeer, Kasenally, & Perkins, 1993) design. For this design $W_1(s)$, the pre-compensator, was chosen as a PI element and the post-compensator $W_2(s)$ was chosen as a low-pass filter. The output-sensitivity and the input co-sensitivity for the longitudinal and lateral controllers are shown in Figs. 8 and 9. The input co-sensitivity plots indicate the controllers have high tolerance of input multiplicative uncertainty, and are hence robust to time delays at the input. The sensitivity plots are quite reasonable except in the yaw channel, which does not roll-off as much as desired at low frequencies; this indicates poor tracking of step inputs.

3.5. 1 DOF loop-shaping controllers

The numerous desirable attributes that $\mathscr{H}^\infty$ loop-shaping controllers McFarlane and Glover (1990) offer, has been one of the driving forces behind its use in the helicopter control context. The method is appealing for practising control engineers, since it allows them to use their intuition and experience.

As an extension of classical loop shaping, the method addresses robust stability and performance objectives simultaneously, by shaping open-loop singular values of the nominal plant with pre/post compensators. In this way, the designer indirectly shapes the closed-loop transfer functions (namely, sensitivity S, and co-sensitivity T) singular values. After an inspection of the singular values of the reduced nominal plant in Fig. 3, and some trials in accordance with the

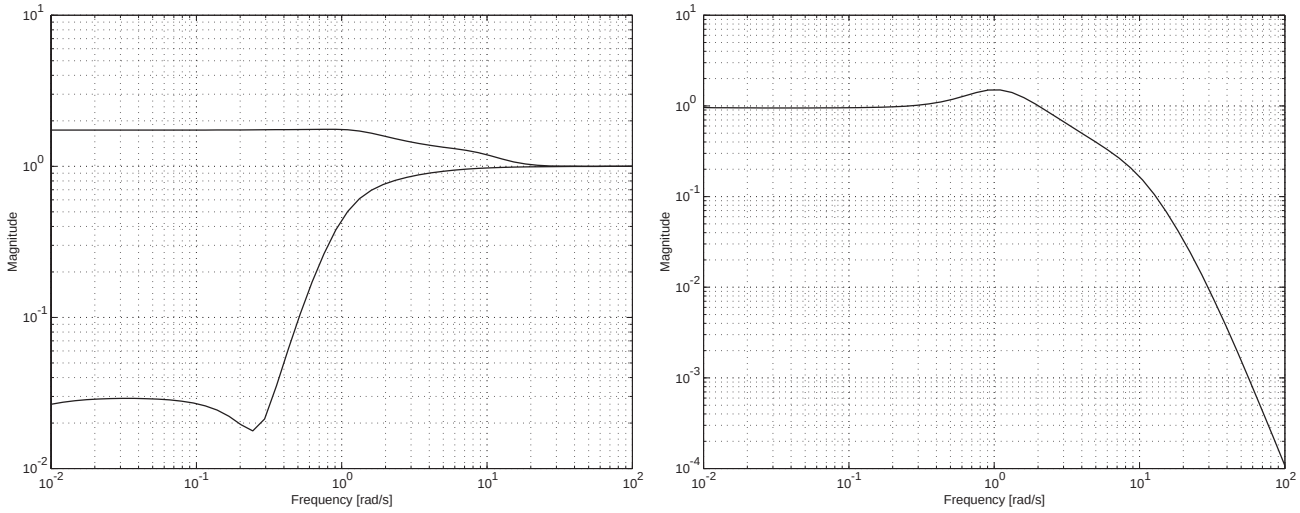

Fig. 8. Longitudinal sensitivities: S_o and T_i.

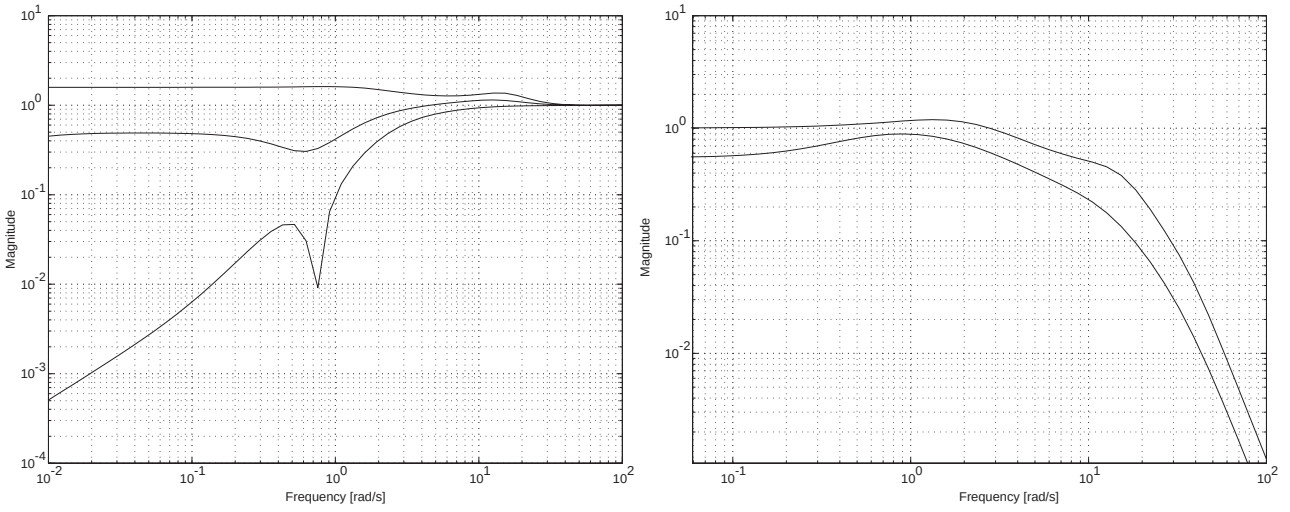

Fig. 9. Lateral sensitivities: S_o and T_i.

loop-shaping procedure guidelines and requirements, each input channel was augmented with a simple PI structured pre-compensator. The integral part was employed to boost low-frequency gain and improve performance (i.e. to ensure $e_{ss} = 0$ when tracking an attitude; good output decoupling; good disturbance rejection at the plant input and output), whereas the proportional part was introduced to rectify the phase-lag added by the integrators at cross-over, to increase robustness and additionally to set the usage authority on the actuators. The diagonally structured post-compensator places an emphasis on the yaw channel by accommodating a low-pass filter with cut-off frequency around the mast rocking mode, aimed for high-frequency roll-off. For ease of tuning of the weighting transfer functions in the structured pre-filter, the control law does not make use of the secondary measurements $(p, q$ rates), which makes the plant square. A sub-optimal (7 per cent) robustly stabilising controller with respect to the normalised coprime factors of the shaped plant G_s was synthesized using the $[K_\infty, \varepsilon_{max}] = \texttt{ncfsyn}(G_s, 1.07)$ command. The achieved stability margin $\varepsilon_{max} = 0.33$ is an indicator that 33 per cent of coprime factor uncertainty is allowed around the cross-over frequency range of the shaped plant. At high and low frequencies, the actual loop shape may differ from the desired one by a factor of $\sqrt{\gamma^2 - 1} = 2.82$.

The frequency responses in Fig. 10 reveal that the system has good disturbance rejection and reference signal tracking at low frequencies with ensured zero steady-state error in all channels except the yaw, and good roll-off at high frequency.

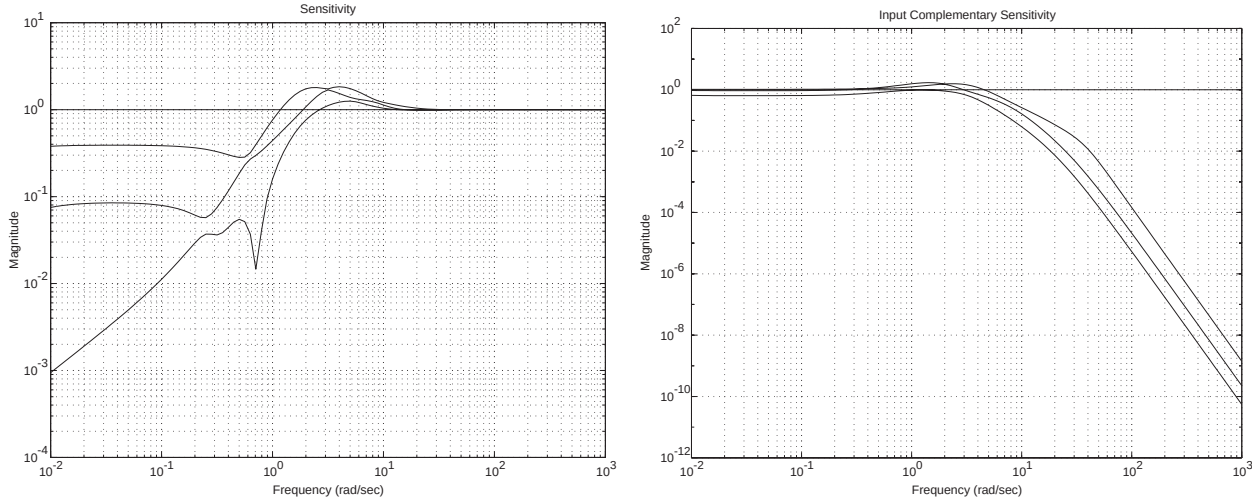

Fig. 10. 1 DOF sensitivities: S_o and T_i.

4. Results

4.1. Controller assessment

The assessment of the $\mathscr{H}^\infty$ controllers described in Section 3 was performed using both nonlinear simulation and flight-testing. The controllers were analysed using traditional control techniques (i.e. observing settling times and overshoots), subjective pilot comments and also elements of the ADS-33 criteria. The ADS-33 (Anonymous, 2000) criteria set out quantitative and qualitative measures of helicopter performance, and many of these criteria have become the de facto standard in recent years.

The ADS-33 classifies *handling qualities* into three levels and 'un-flyable':

- *Level* 1, the most desirable corresponds to flying qualities which require no improvement;
- *Level* 2, the pilot has desirable/adequate control of the vehicle, but the handling of the aircraft still requires improvement; and
- *Level* 3 corresponds to undesirable flying qualities, although the pilot is still in control of the helicopter.

These handling qualities can be assessed quantitatively, using measured or simulated data, or more qualitatively using pilot comments in conjunction with precisely formulated scales. In this paper, we use the ADS-33-defined short-term bandwidth and phase delay parameters to assess the controllers objectively on an axis-by-axis basis. It is important to emphasise that the ADS-33 definition of bandwidth is at odds with the conventional definition: bandwidth, when measuring attitudes, is defined as the frequency at which the phase crosses -135°; phase delay is, roughly, how rapidly the phase changes at frequencies beyond the bandwidth. For a more thorough description of these concepts (see Anonymous, 2000). Note that bandwidths and phase-delays can be calculated from simulation data and hence can be used to predict, to some extent, the in-flight performance of the helicopter.

This paper also contains some handling qualities information imparted by pilots. Pilots rate the performance of an aircraft in terms of handling qualities ratings (HQRs). Low HQRs indicate a helicopter with good handling qualities: HQRs from 1–3 are used to indicate *Level* 1 performance; HQRs of 4–6 indicate *Level* 2 performance; and 7–9 indicate *Level* 3 performance. Most current helicopters do not perform to *Level* 1 standard and it is rare for pilots to award HQRs of 2 or better. There is a stark divide on the border of *Level* 1 where, if in doubt, pilots tend to award HQRs of 4 rather than 3 (which requires no improvement).

4.2. Nonlinear simulations

In the past, $\mathscr{H}^\infty$ controllers tested in the flights associated with the papers Postlethwaite et al. (1999) and Walker et al. (1999) were not always guaranteed to give stable closed loops in flight; controllers which appeared to behave well in simulation sometimes behaved very unpredictably in flight. Part of this was perhaps due to the fidelity of some of the older models used, and an incorrect use of a scaling matrix which has recently been discovered. Another possible explanation is the "ideal" nature of the simulations: no gains or parameters were varied from their nominal, although various trim-points were tested successfully.

In order to address this issue several "crude" alterations were made to assess robustness through simulation. The most salient of these improved simulation techniques was assessment of worst-case time-delay tolerances: all controllers were tested to computational delay tolerances of 80 mS, when the actual delay was

estimated at roughly half this value. In addition, controllers were subjected to simulations in which the open-loop aircraft gain was increased by a factor of 1.4 across all frequencies; this test crudely mimicked some of the open-loop gain uncertainty. All controllers which performed satisfactorily in simulation for these two robustness "criteria" performed satisfactorily in flight.

4.2.1. Full-information feedforward with the PI feedback regulator

Figs. 11 and 12 show the nonlinear responses to a -0.2 rad step-like demand with a rate limit of 0.2 rad/s in roll and pitch, respectively. We can see that the responses with the feedforward filter are remarkably better than those given by the PI regulator alone in Fig. 6. The on-axis transient responses are generally good: little overshoot, fast responses except in pitch which is too slow, prompt attitude capture and good separation of controls. However, the controller suffers from a slow lateral drift. This drift is due to the poor regulation performance of the PI controller which cannot ensure tracking robustness (not enough closed-loop gain). In many situations, the pilot can compensate manually for this drift at the expense of additional workload which can prove prohibitive during more aggressive or complex manoeuvres.

4.2.2. De-coupled controllers

Figs. 13 and 14 show the response to step-like demands in roll and pitch, respectively, using the full augmented nonlinear simulation. Observe that the on-axis responses are generally good with little overshoot and sharp, accurate attitude capture. There is little off-axis coupling; it always remains under 20 per cent. For larger, sharper demands the responses can deteriorate, with more coupling and poorer transient behaviour, but this was not thought excessive.

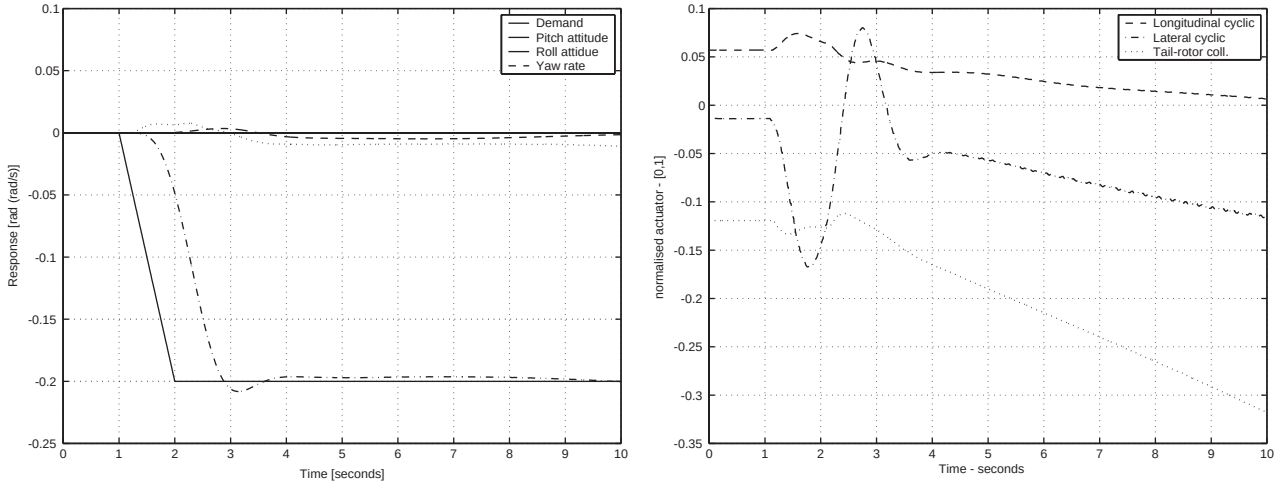

Fig. 11. Responses to a step in roll (PI feedforward).

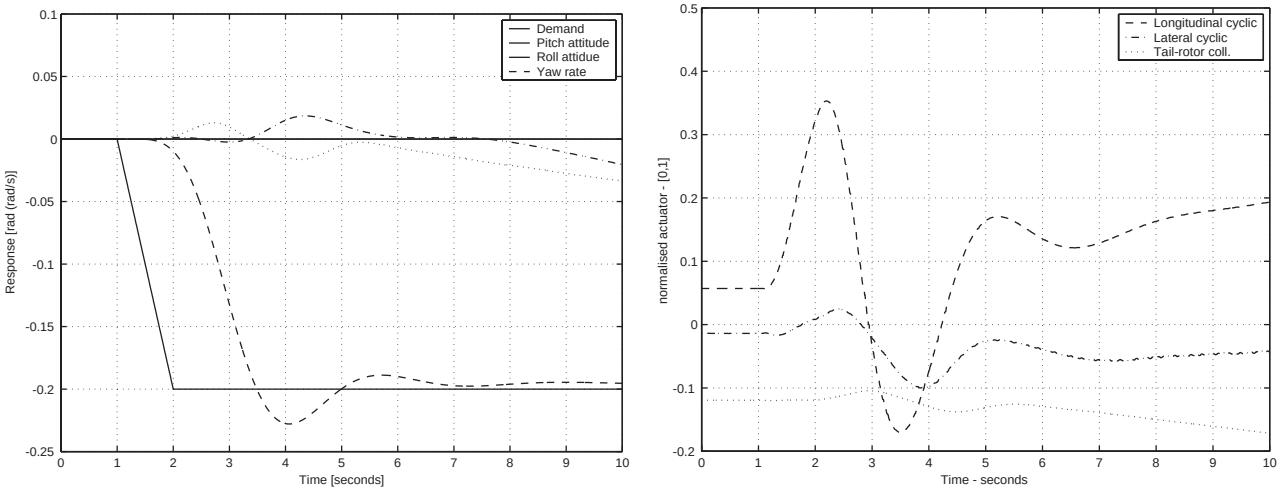

Fig. 12. Responses to a step in pitch (PI feedforward).

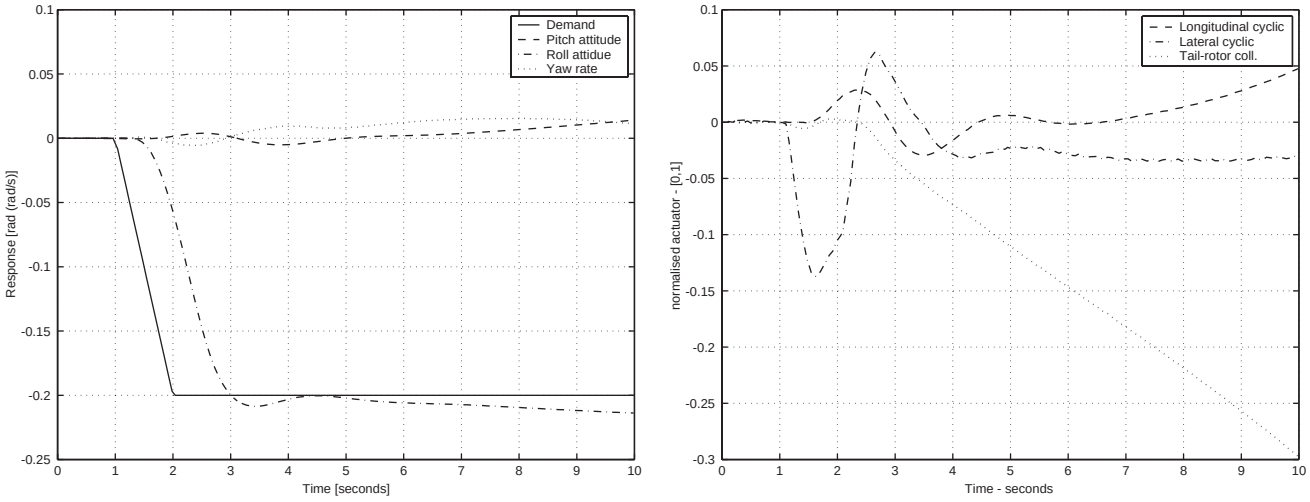

Fig. 13. Response to a step in roll attitude (decoupled).

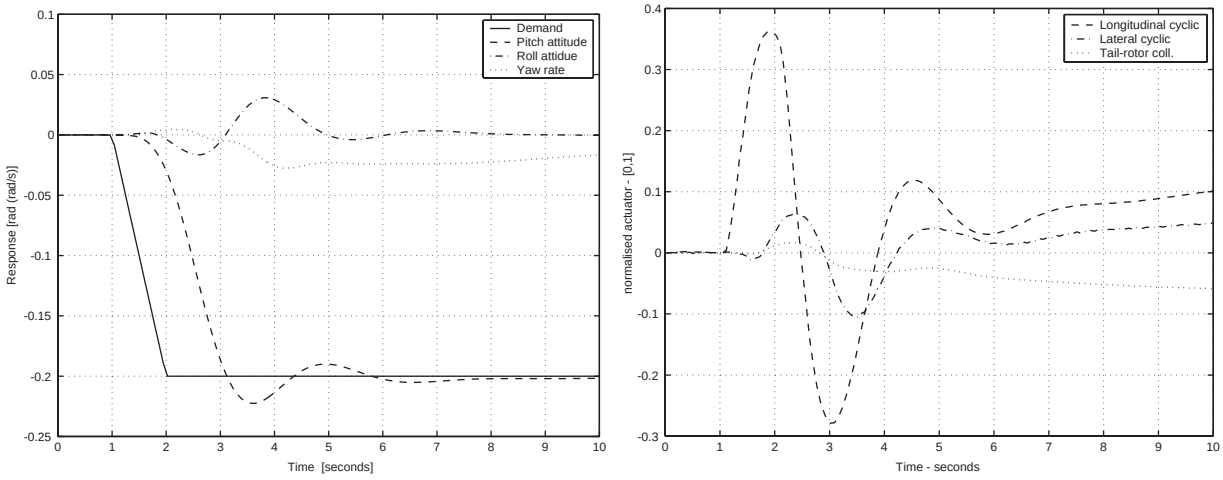

Fig. 14. Response to a step in pitch attitude (decoupled).

4.2.3. 1 DOF loop-shaping controllers

Figs. 15 and 16 show the closed-loop time responses to a step-like demand of -0.2 rad with a rate-limit of 0.2 rad/s in the roll and pitch channels, respectively. Despite the lateral oscillations which can be seen in Fig. 12, the design method provides acceptable decoupling between controlled channels. However, note the slow rise time in pitch attitude response that resulted, in flight test, in a pilot-induced-oscillation tendency. Table 4 shows that the closed-loop bandwidth should be increased for desirable handling qualities. To rectify this, in future designs a pre-filter may be introduced to facilitate model matching with an ideal response type.

4.3. Flight test results

The three flight tests were carried out over 2 days with little time to iterate on designs; approximately 2–3 h of flight test data were gathered in total. With good visibility and light winds, weather conditions provided an adequate and favourable environment to perform handling qualities testing, ultimately leading to ADS-33 UCE 1 (Usable Cue Environment of 1).

The following contains extracts from the flight tests. The frequency responses were generated using the transfer function estimate (`tfe`) command in the Matlab Signal Processing toolbox, using overlapping Hanning windows and data filtered through a 10 Hz cut-off, second-order Butterworth filter.

4.3.1. PI + $\mathscr{H}^\infty$ feedforward

Fig. 17 shows a pulse in roll attitude applied to the helicopter at hover. Fig. 18 shows the frequency responses computed from flight test frequency sweeps. Note that only the lateral channels have been tuned to get reasonably fast responses. The pitch channel response results from a previous tuning which was deliberately low bandwidth. In a precision hover manoeuvre the pilot gave an HQR of 4.5, which corresponds to solid *Level* 2 handling qualities. Stated

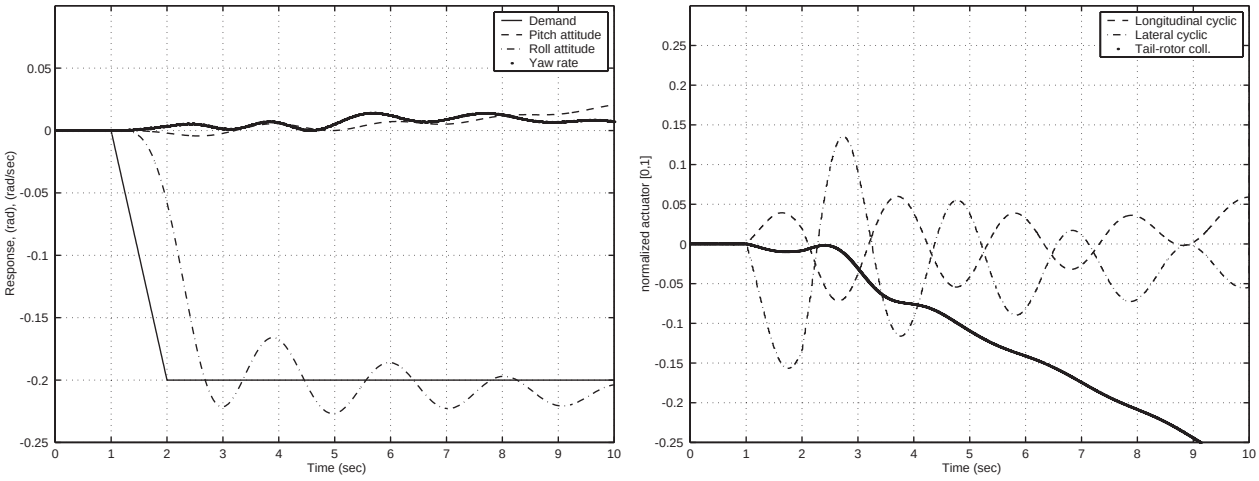

Fig. 15. Response to a step in roll attitude (1 DOF).

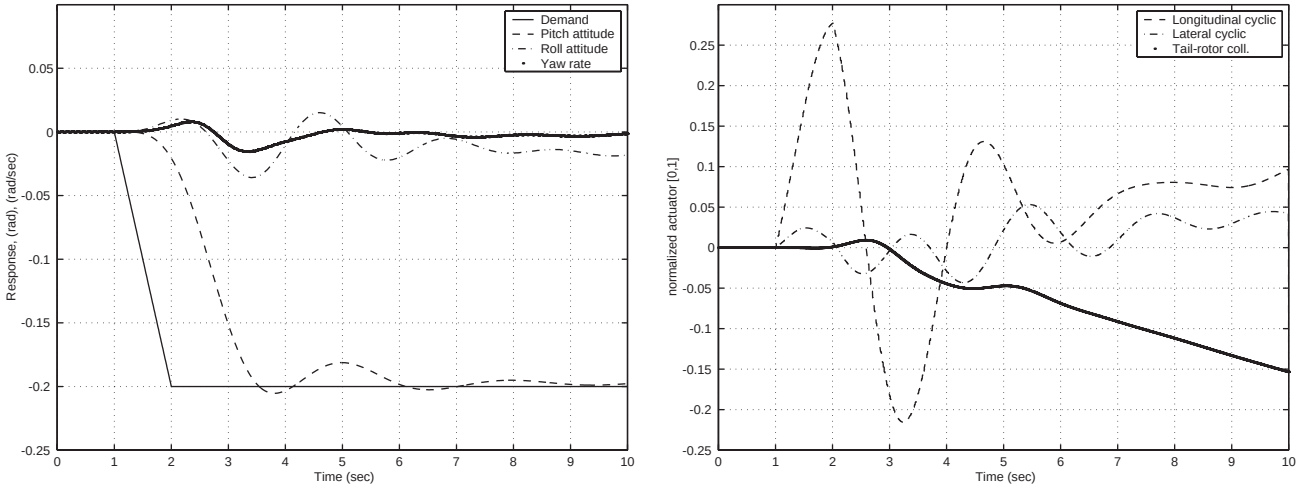

Fig. 16. Response to a step in pitch attitude (1 DOF).

Table 4
Handling qualities

Controller	B/W	P/D	Handling quality		
			Combat	Other	UCE = 1
Pitch					
Full inf.	1.6 (2.2)	0.23 (0.29)	2	2	1
Decoup.	2.1 (2.3)	0.15 (0.12)	1	1	1
1 DOF	2.37 (2.01)	0.25 (0.09)	2	2	1
Roll					
Full inf.	3.1 (3.3)	0.23 (0.21)	2	1	1
Decoupled	3.3 (3.1)	0.07 (0.07)	2	1	1
1 DOF	3.17 (3.3)	0.11 (0.06)	2	1	1
Yaw					
Full inf.	4.64 (4.8)	0.08 (0.1)	1	1	N/a

another way, this means that the handling qualities were *desired* but the workload from the pilot was reasonably high (and therefore not a true HQR 4).

4.3.2. De-coupled controllers

Fig. 19 depicts a pulse in roll applied to the helicopter at hover. Note the crisp attitude capture and negligible overshoot. The pilot was satisfied with the pitch and roll channels although he observed some, but not excessive, cross-coupling between the two. He did however find yaw quite sluggish. In the *precision hover* manoeuvre the pilot gave an HQR of 3, which corresponds to *Level* 1 handling qualities. Unfortunately, time did not allow any other manoeuvres to be performed.

Fig. 20 shows the frequency responses from demand to attained attitude in the roll and pitch channels, respectively. Observe that both channels show smooth frequency responses.

4.3.3. 1 DOF loop-shaping controllers

Fig. 21 illustrates 3 pulse demands in the roll channel in the helicopter at hover. Note the consistency of oscillations in nonlinear simulation and flight test results of roll attitude channel. The only manoeuvre that was

subject to pilot rating was *precision hover*, rated 5 on the HQR scale, corresponding to *Level* 2 flying qualities.

4.4. ADS-33 evaluation

Table 4 shows the bandwidths, phase delays and handling quality level induced in the aircraft by the three controllers, calculated according to the ADS-33 criteria. The unbracketed figures are the results from calculations from flight-test data; the bracketed figures are predictions using linear models. Note the strong similarity between the predicted and achieved ratings. The final three columns in the table denote the corresponding level of handling quality the controllers delivered according to the ADS-33 document. Note that this is dependent on the type of task the pilot is performing, combat being the most demanding.

Figs. 22 and 23 depict the calculated ADS-33 handling qualities for the pitch and roll channels in the combat/target tracking scenario (the most demanding environment). The arrows connecting the points indicate the direction in which the handling qualities move from simulation to flight test. Note that the handling qualities are remarkably similar for both simulation and flight test, suggesting both reasonably accurate models and robust controllers.

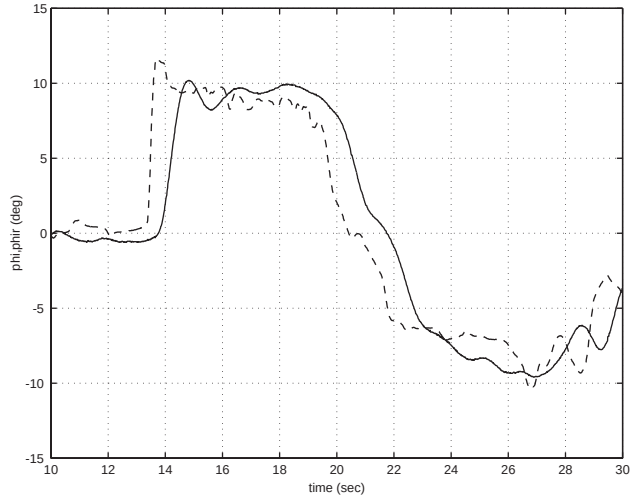

Fig. 17. Step in roll attitude (PI + $\mathscr{H}^\infty$ feedforward): dashed—demand; solid—response.

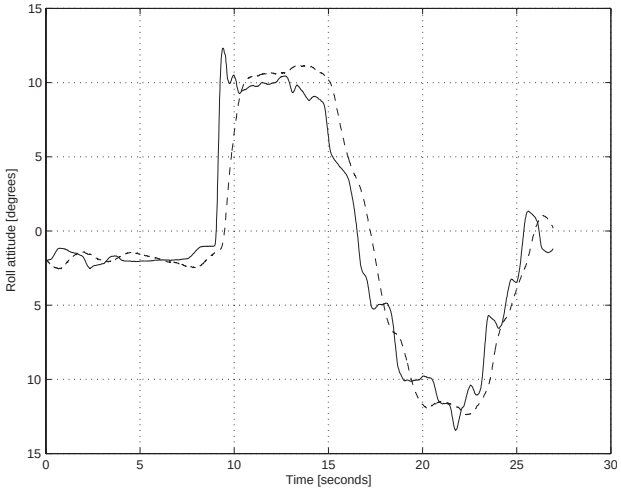

Fig. 19. Step in roll attitude (decoupled): solid—demand; dashed—response.

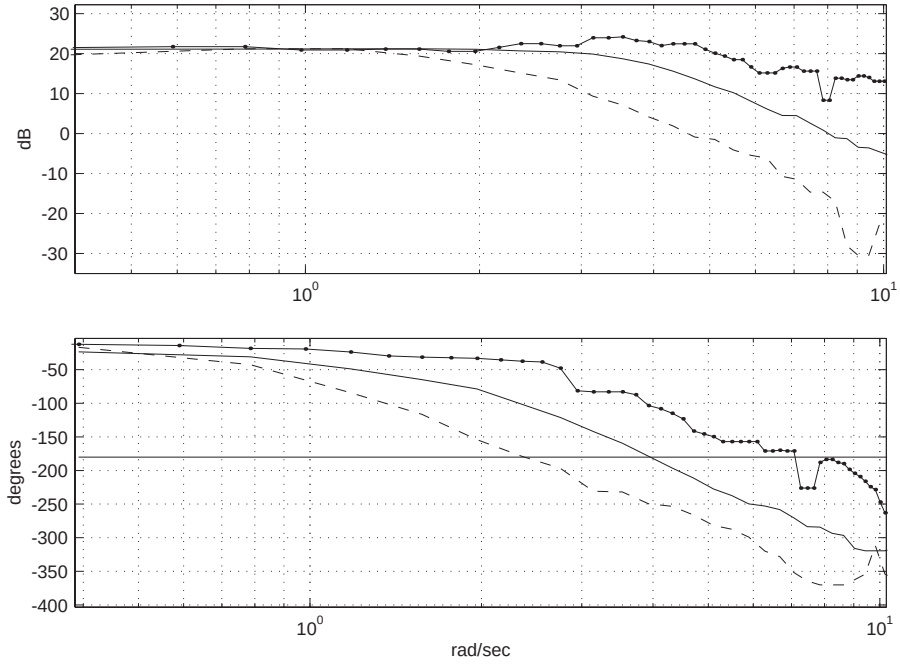

Fig. 18. On-axis frequency sweeps; PI + $\mathscr{H}^\infty$ feedforward (solid: roll, dashed: pitch, dotted: yaw).

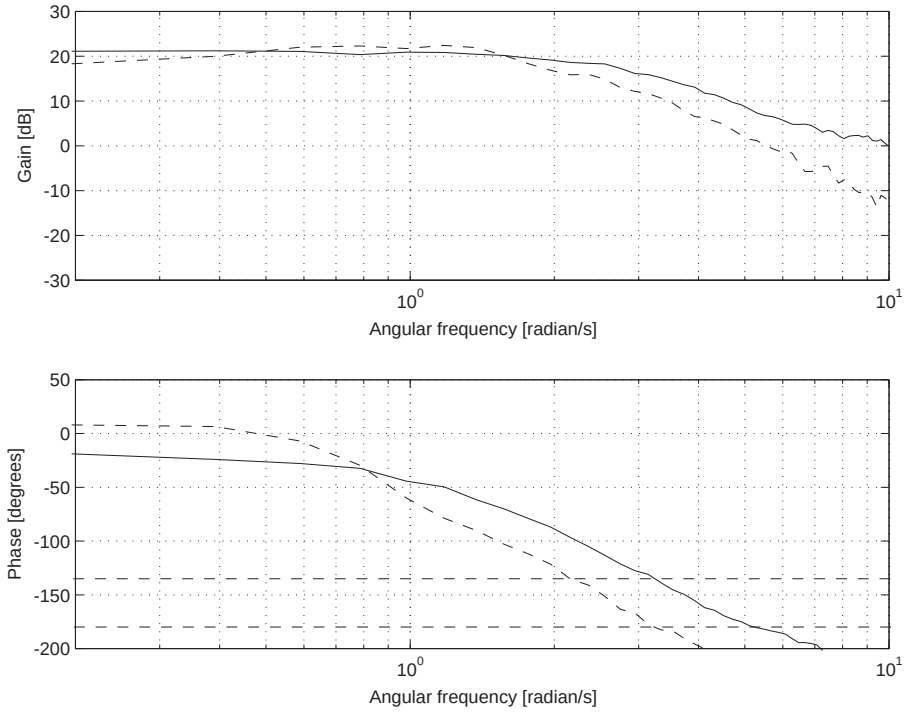

Fig. 20. On-axis frequency sweeps; decoupled (solid—roll; dashed—pitch).

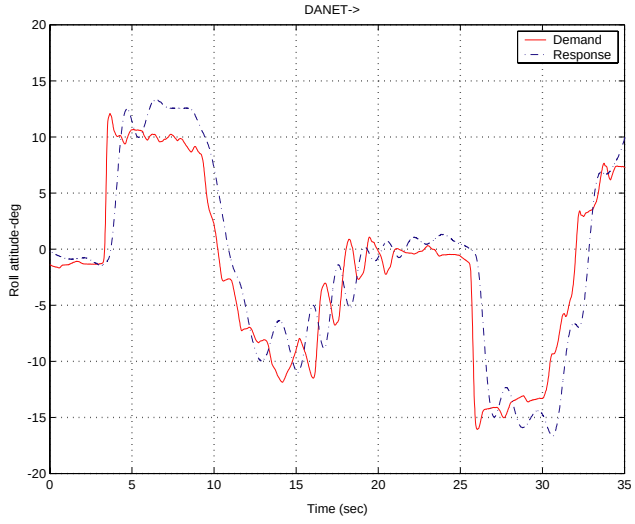

Fig. 21. Step in roll attitude (1 DOF).

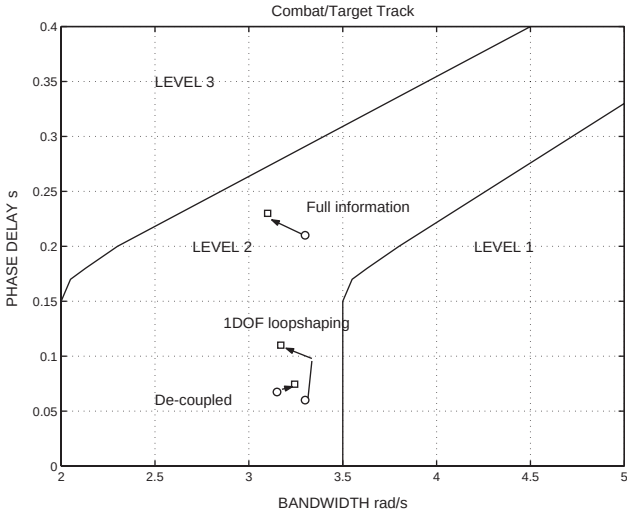

Fig. 22. ADS-33 plot of roll performance.

5. Conclusion

5.1. Current status

This paper has described the design and flight testing of several different $\mathscr{H}^\infty$ controllers. Although flight testing was conducted over only 2 days, the controllers induced a mixture of adequate and desirable handling qualities in the helicopter, depending on manouevre and controller. The small difference between predicted and achieved bandwidths was encouraging and pointed towards good model fidelity and robust controllers. One of the notable outcomes of the trial was that, despite the multivariable nature of the plant, cross-coupling between axes was relatively low and therefore confirms the applicability of $\mathscr{H}^\infty$ to multivariable systems. Also, there was not a significant difference in cross-coupling between the multivariable and de-coupled controllers, which suggests that, at least with the current model fidelity, it is not *necessary* to

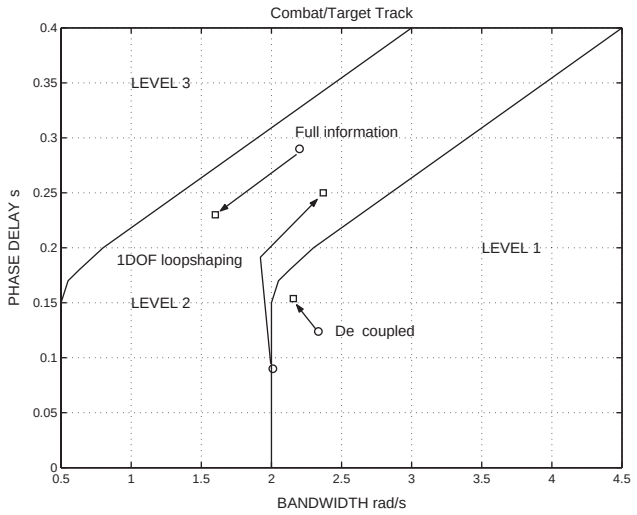

Fig. 23. ADS-33 plot of pitch performance.

work with de-coupled designs, although they can be easier to tune.

This flight test concentrated on a "cautious" approach to controller design, whereby robustness was the primary focus; another flight test is planned in the future where the $\mathscr{H}^\infty$ controllers will be re-tuned to increase performance. One of the interesting outcomes of the flight tests described here was the quite delicate balance between a control law which was too sluggish and one which was too fast. From pilot comment it was clear that neither a slightly overdamped response nor a slightly too active response was desirable. In addition, an excessively active control signal excited unmodelled dynamics (such as mast-rocking and flexible modes) which, although not detrimental to the primary response of the aircraft, led to degraded handling qualities ratings due to a "choppy" ride.

5.2. Future work

The flight tests described in this paper were carried out in the summer of 2001 and since then two further sets of flight tests have been performed. In certain respects the controllers tested in these flight tests performed better than the ones described here: the bandwidths of these controllers were increased (reaching around 4 rad/s in roll) and the handling qualities reported by the pilots were better for low aggression manoeuvres (the controllers routinely yielded HQR 3—*Level* 1—ratings in the precision hover and pirouette manoeuvres). However, these results were marred by faulty actuation and sensing and hence do not stand up to scientific scrutiny. In particular, a gain in the pitch rate gyroscope was poorly scaled, at twice its nominal value, leading to a much too slow rate build-up. This we suspect is the source of the "sluggish and overdamped" response in the pitch axis which the pilots complained of when performing high aggression manoeuvres.

From a certain perspective even these tests were successful in that $\mathscr{H}^\infty$ controllers could stabilise and produce at least satisfactory, and even desirable, performance on an aircraft which, in effect, was quite different to that described by the model used for the design.

Future flight tests are planned to improve performance further and produce desirable HQR's. The main focus will be on the design of control laws which are sufficiently fast for desirable performance, yet produce less active control signals in order to improve ride quality.

Acknowledgements

The authors would like to thank S. Howell and A. McCallum from QinetiQ (formerly DERA) Bedford for helpful discussions regarding the Bell 205 model and flight tests. Thanks are also due to the pilots R. Erdos and S. Carignan, of the NRC Flight Research Labs, Ottawa, for useful comments.

References

Anonymous, (2000). *Handling qualities requirements for military rotorcraft, aeronautical design standard ADS-33E-PRF*. U.S. Army Aviation and Missile Command, Aviation Engineering Directorate, Redstone Arsenal, Alabama.

Baillie, S. W., Morgan, M. J., & Goheen, K. (1995). Practical experiences in control system design using the NRC Bell 205 airborne simulator. *AGARD conference proceedings 560, actice control technology: applications and lessons learned* (pp. 27.1–27.12).

Gubbels, A. W., & Goheen, K. R. (1997). Digital re-design of the Bell 205 airborne simulator artificial feel system. *Canadian Aeronautics and Space Journal*, *43*(1), 57–68.

Hoh, R. H., Mitchell, D. G., & Aponso, B. L. (1989). *Background information and user's guide for handling requirements for military rotorcraft*. USAAVSCOM technical report 89-A-008.

Howell, S., & McCallum, A. (2001). Private communication.

Limebeer, D. J. N., Kasenally, E. M., & Perkins, J. D. (1993). On the design of robust two-degree-of-freedom controllers. *Automatica*, *29*(1), 157–168.

McFarlane, D. C., & Glover, K. (1990). *Robust controller design using normalised coprime factor plant descriptions*. In *Lecture notes in control and information sciences*, Vol. 138. Berlin: Springer.

McVicar, J. S. G., & Bradley, R. (1997). Efficient and robust algorithms for trim and stability analysis of advanced rotorcraft simulations. *The Aeronautical Journal*, *10*, 375–387.

Padfield, G. D. (1981). *A theoretical model of helicopter flight mechanics for application to piloted simulation*. Technical report RAE TR 81048, Royal Aircraft Establishment, Farnborough.

Padfield, G. D. (2000). *Helicopter flight dynamics: The theory and application of flying qualities and simulation modelling*. UK: Blackwell Science Ltd.

Peters, D., & HaQuang, N. (1988). Dynamic inflow for practical applications. *Journal of the American Helicopter Society*, *33*(4), 64–68.

Postlethwaite, I., Smerlas, A., Walker, D. J., Gubbels, A. W., Baillie, S. W., Strange, M. E., & Howitt, J. (1999). $\mathscr{H}^{\infty}$ control of the NRC Bell 205 fly-by-wire helicopter. *Journal of the American Helicopter Society*, *44*(4), 276–284.

Prempain, E., & Postlethwaite, I. (2001). Feedforward control: A full information approach. *Automatica*, *37*(1), 17–28.

Prouty, R. W. (1995). *Helicopter performance, stability and control*. Malabar, FL, US: Krieger Publishing.

Skogestad, S., & Postlethwaite, I. (1996). *Multivariable feedback control: Analysis and design*. Chichester, UK: Wiley.

Strange, M. E., & Howitt, J. (1998). *The configuring of HELISIM to represent the flight dynamics of the NRC Bell 205 helicopter*. DERA internal report.

Tombs, M. S. (1987). *Robust control system design with application to high performance helicopters*. Ph.D. thesis, University of Oxford.

Walker, D. J., & Postlethwaite, I. (1996). Advanced helicopter flight control using two-degree-of-freedom $\mathscr{H}^{\infty}$ optimisation. *AIAA Journal of Guidance Control and Dynamics*, *19*(2), 461–468.

Walker, D. J., Turner, M. C., Smerlas, A., Gubbels, A. W., & Strange, M. E. (1999). Robust control of the longitudinal and lateral dynamics of the Bell 205 helicopter. *Proceedings of the American Control Conference*, San Diego, USA, Vol. 4 (pp. 2742–2726).

Yue, A., & Postlethwaite, I. (1990). Improvement of helicopter handling qualities using $\mathscr{H}^{\infty}$ optimisation. *IEE Proceedings-D Control Theory and Applications*, *137*(2), 115–129.